Proceedings of the 17th World Congress
The International Federation of Automatic Control
Seoul, Korea, July 6-11, 2008

Successive Linearization-based Stochastic Repetitive Control Technique and its Applications to SMB and CATOFIN Processes

Kwang Soon Lee *, **Woohyun Yun** *, **Wangyun Won** *
Jay H. Lee **

* *Department of Chemical and Biomolecular Engineering, Sogang University, Seoul, Korea (Tel: 82-2-705-8477; e-mail: kslee@sogang.ac.kr)*
** *School of Chemical and Biomolecular Engineering., Georgia Institute of Technology, GA, USA*

Abstract: A repetitive control technique which is based on a time-varying stochastic state space model obtained by cycle-to-cycle linearization of a nonlinear fundamental process model around the operation trajectories in the previous cycle is introduced. The control technique was applied to two repetitive chemical processes: simulated moving bed, a continuous chromatograph separation process, and CATOFIN process, a catalytic propane dehydrogenation reactor where dehydrogenation and coke oxidation alternate over short periods. Numerical studies have shown that the proposed RC techniques are very effective in improving the operation of both processes.

Keywords: repetitive control; SMB process; CATOFIN process; stochastic control

1. INTRODUCTION

Repetitive control (RC) has a ground on the notion that the operation of a repetitive system can be improved by cycle-wise feedback of the output error to the input calculation for the upcoming cycle. The idea of RC was first proposed by Inoue et al. [1981] and has reached maturity by Omata et al. [1984] and Hara et al. [1988] for the SISO continuous-time system. Later, Weiss and Häfel [1999] extended the approach to the MIMO continuous-time system. Discrete-time RC methods have also been investigated after the first contribution by Tomizuka et al. [1988] as reviewed by Longman [2000]. Basically the methods mentioned above have been based on the internal model principle and proposed for the time-invariant linear system. Lee et al. [2001a] have suggested various optimal RC methods for the linear time-varying system with a new interpretation that the RC action is cycle-wise integral control. A state space model that describes the cycle-wise state transition was constructed using the lifting technique, and RC laws that minimize quadratic optimal criteria with and without real-time feedback were presented.

As an extension of Lee et al. [2001a]'s work, in this study, stochastic RC methods that are based on successive linearization of a nonlinear physical model is presented, especially aiming at repetitive chemical processes, which are typically nonlinear and very often subject to drifting disturbances with large model error. In the construction of the RC methods, a time-varying stochastic linear state space model was derived first from the linearization of the nonlinear process model around the operation trajectories after each cycle, and the decomposition of the uncertainty terms into cycle-wise correlated and uncorrelated parts. Then optimal control laws with quadratic criteria were applied. After necessary tailoring to each process, the RC methods have been implemented on two repetitive chemical processes: simulated moving bed (SMB) a continuous chromatograph separation process, and CATOFIN process, a catalytic propane dehydrogenation reactor where dehydrogenation and coke oxidation alternate over short periods. Numerical studies have shown that the proposed RC techniques are very effective in improving the operation of both processes despite large model uncertainty and unpredicted disturbances.

2. LINEARIZATION-BASED STOCHASTIC RC METHOD

2.1 Construction of linear stochastic model

We consider a nonlinear stochastic discrete-time process

$$\begin{aligned} x(t+1) &= f(x(t), u(t)) + \bar{d}(t) \\ y(t) &= c(x(t)) + \hat{d}(t) \end{aligned} \tag{1}$$

where $\bar{d}$ and $\hat{d}$ refer to zero-mean random disturbances. Let the output reference trajectory $r(t)$ be periodic with the period N. If the process at the k^{th} cycle is linearized around the operation trajectory at the $k-1^{\text{th}}$ cycle, we have

$$\begin{aligned} x_k(t+1) &= \bar{A}_{k-1}(t)x_k(t) + \bar{B}_{k-1}(t)u_k(t) + m_k(t) \\ y_k(t) &= \bar{C}_{k-1}(t)x(t) + n_k(t), \quad x_k(0) = x_{k-1}(N) \end{aligned} \tag{2}$$

978-1-1234-7890-2/08/$20.00 © 2008 IFAC 10.3182/20080706-5-KR-1001.3229

where $x_k(0) = x_{k-1}(N)$ represents the continuous transition of the state from one cycle to the next. In the above, m and n include not only the disturbances but also model error. Both m and n have cycle-wise repeated part (mostly from the model error) and cycle-wise random part. Thus m and n can be represented as

$$m_k(t) = \bar{m}(t) + \hat{m}_k(t) \tag{3}$$

and similarly for $n_k(t)$. In the above, $\bar{m}(t)$ is a deterministic signal and $\hat{m}(t)$ represents a zero mean i.i.d. process in t as well as k. Eq. (2) can be decomposed into two parts, the pure stochastic part that is driven by $\hat{m}(t)$ and $\hat{n}(t)$ with no input

$$\begin{aligned} \hat{x}_k(t+1) &= \bar{A}_{k-1}(t)\hat{x}_k(t) + \hat{m}_k(t) \\ \hat{y}_k(t) &= \bar{C}_{k-1}(t)x_k(t) + \hat{n}_k(t) \end{aligned} \tag{4}$$

and the deterministic part that is driven by $\bar{m}(t)$, $\bar{n}(t)$, and $u(t)$. By taking the cycle-wise difference of the latter part under the assumption that $\bar{A}_{k-1}(t) \approx A_{k-2}(t)$ and similarly for $\bar{B}_{k-1}$ and $\bar{C}_{k-1}$, both $\bar{m}(t)$ and $\bar{n}(t)$ are eliminated and the following relationship is obtained:

$$\begin{aligned} \Delta\bar{x}_k(t+1) &= \bar{A}_{k-1}(t)\Delta\bar{x}_k(t) + \bar{B}_{k-1}(t)\Delta u_k(t) \\ \bar{y}_k(t) &= \bar{y}_{k-1}(t) + \bar{C}_{k-1}(t)\Delta\bar{x}_k(t) \end{aligned} \tag{5}$$

where $\Delta x_k(t) \triangleq x_k(t) - x_{k-1}(t)$ and $\Delta u_k(t) \triangleq u_k(t) - u_{k-1}(t)$. By noting that $y_k(t) = \hat{y}_k(t) + \bar{y}_k(t)$, (4) and (5) can be combined to form the following stochastic state space model:

$$\begin{aligned} z_k(t+1) &= A_{k-1}(t)z_k(t) + B_{k-1}\Delta u_k(t) + w_k(t) \\ y_k(t) &= C_{k-1}(t)z_k(t) + v_k(t) \end{aligned} \tag{6}$$

where $z_k(t) \triangleq [\hat{x}_k(t)^T \ \Delta\bar{x}_k(t)^T \ \bar{\mathbf{y}}_{k-1}^T]^T$, $\bar{\mathbf{y}}_{k-1} = [\bar{y}_{k-1}(1)^T \cdots \bar{y}_{k-1}(N)^T]^T$, $w_k(t)^T \triangleq [\hat{m}_k(t)^T \ 0 \cdots 0]$, and so forth. More details on the above derivation can be refered to Lee et al. [2001a] and Lee et al. [2001b].

2.2 Quadratic RC methods

For the state space model in (6), the following one-cycle-ahead quadratic optimal control problem can be considered:

$$\min_{\Delta u_k(\cdot)} \frac{1}{2}\sum_{t=1}^{N} \|e_k(t+1|t)\|^2_{Q(t)} + \|\Delta u_k(t)\|^2_{R(t)} \tag{7}$$

where $e_k(t+1|t) \triangleq r(t+1) - y_k(t+1|t)$ and $y_k(t+1|t)$ represents the optimal prediction of $y_k(t+1)$ on the basis of the information up to t at the k^{th} cycle. $y_k(t+1|t)$ is obtained as a function of $\Delta u_k(t)$ using the Kalman filter for (6).

$$\begin{aligned} z_k(t|t) &= z_k(t|t-1) + K(t)(y_k(t) - C_{k-1}(t)z_k(t|t-1)) \\ z_k(t+1|t) &= A_{k-1}(t)z_k(t|t) + B_{k-1}(t)\Delta u_k(t) \\ y_k(t+1|t) &= C_{k-1}(t)(A_{k-1}(t)z_k(t|t) + B_{k-1}(t)\Delta u_k(t)) \end{aligned} \tag{8}$$

Note that the state estimate is carried over to the cycle boundary according to $x_{k+1}(0) = x_k(N)$. $K(t)$ represents the cycle-wise steady state time-varying Kalman gain.

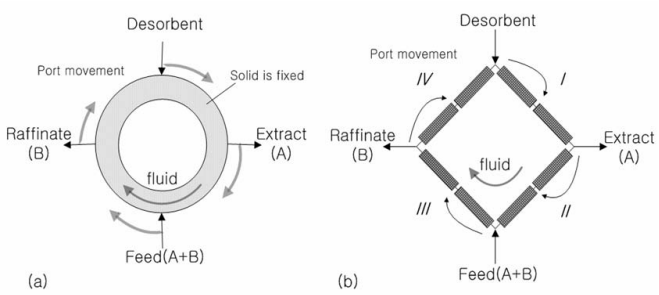

Fig. 1. A four-zone SMB system.

$K(t)$ can be obtained from the steady state Kalman filter for the lifted equation of (6) over a cycle. Details can be found in Lee et al. [2001a]. The above is a standard finite-time optimal tracking problem. Since N is finite, the above problem is solvable with and without constraints.

Eq. (8) can be generalized to include the summation over the cycle index.

$$\min_{\Delta u_k(\cdot)} \frac{1}{2}\sum_{k=1}^{M}\left[\sum_{t=1}^{N} \|e_k(t+1|t)\|^2_{Q(t)} + \|\Delta u_k(t)\|^2_{R(t)}\right] \tag{9}$$

In this research, only the one-cycle-ahead optimal control problem was considered.

3. APPLICATION TO SMB PROCESS

3.1 Description of process and control problem

The SMB is a rather complicated process where continuous material flow and discrete pot switching are combined. The principle of SMB can be understood from the hypothetical circular chromatography with continuous port moving as shown in Fig. 1(a), which is a redrawing of a true moving bed (TMB) by fixing the bed but moving the ports instead. In this system, the feed (A+B) is separated as in the usual chromatography. A and B move along the desorbent flow and are split by different affinities with the adsorbent. If the ports are rotated in the same direction of the desorbent flow with the average moving speed of the feed components, the stronger affinity component (A) can be removed from the extract port while the weaker affinity one (B) can be withdrawn from the raffinate port under continuous feeding and product removal. Fig. 1(b) shows a scheme of the SMB where the circular bed and the continuous port moving are replaced by several disjoint columns and discrete port switching. As the number of columns is increased, the SMB can be closer to the TMB. In this study, a four zone SMB with eight identical columns as shown in Fig. 1(b) is considered. Obviously, the SMB is a typical repetitive process.

The SMB process has extract and raffinate concentrations as the output variables and three flow rates as manipulable input variables. In this study, the control objective was chosen to steer the extract and raffinate purities averaged over a switching cycle to respective target values by manipulating two flow rates while satisfying input constraints.

3.2 Process model

Dynamics of a single SMB column can be described by a set of partial differential equations (PDE's) for the concentrations of A and B in the fluid and adsorbed phases along the axial direction. Therefore, the total process is described by 32 (2 components in 2 phases in 8 columns) PDE's. The PDE model was reduced to an ordinary differential equation (ODE) model in time by applying the cubic spline collocation method (CSCM) (Yun and Lee, 2007). The resulting ODE model could represent the original PDE model with much higher accuracy than the ordinary orthogonal collocation-based ODE model. After incorporating the column switching logic, the final ODE model was obtained in the following form:

$$\frac{dq(t)}{dt} = F(u(t))q(t) + G(u(t)), \quad t \in [0,T] \tag{10}$$
$$p(t) = H(q(t)) \triangleq \left[\frac{c_A}{c_A + c_B}\Big|_{\text{ext}} \quad \frac{c_B}{c_A + c_B}\Big|_{\text{raf}} \right]^T$$
$$y(t) = \frac{1}{t}\int_0^t p(\tau)d\tau$$

where q denotes the state vector composed of the fluid and adsorbed phase concentrations of A and B at the collocation points in the eight columns; $u \triangleq [Q_I \;\; Q_{II}]^T$, flow rates in zones I and II in Fig. 1(b); T is the column switching period. The above ODE was used as the numerical process in the simulation study.

3.3 RC formulation

For RC design, the zero-order hold discrete-time equivalent model for (10) was obtained first such that

$$q_k(t+1) = A(u_k(t))q_k(t) + B(u_k(t)) \tag{11}$$
$$y_k(t) = \frac{1}{N}\sum_{i=1}^{t} H(q_k(i)) = y_k(t-1) + H(q_k(t))$$

where $A(u_k(t)) \triangleq e^{F(u_k(t))h}$, $B(u_k(t)) \triangleq F^{-1}(u_k(t))[e^{F(u_k(t))h} - I]G(u_k(t))$; h denotes the sampling interval. By augmenting the state to $x_k(t) \triangleq [q_k(t)^T \; y_k(t-1)^T]^T$, (11) can be converted to

$$x_k(t+1) = \bar{A}(u_k(t), x_k(t))x_k(t) + \bar{B}(u_k(t)) \tag{12}$$
$$y_k(t) = \bar{H}(x_k(t))$$

Linearizing the above equation around the operation trajectories at the $k-1^{\text{th}}$ cycle and incorporating uncertainties in additive terms yields a time-varying linear stochastic model as in (2). Following the procedure described in the previous section, we obtained the model equation as given in (6).

It was assumed that the average concentrations are measured only at the end time of each cycle. Accordingly, the quadratic objective was modified to

$$\min_{\Delta u_k(\cdot)} \frac{1}{2}\left\{ \|r - y_{k|k-1}(N)\|_Q^2 + \sum_{t=0}^{N-1} \|\Delta u_k(t)\|_R^2 \right\} \tag{13}$$

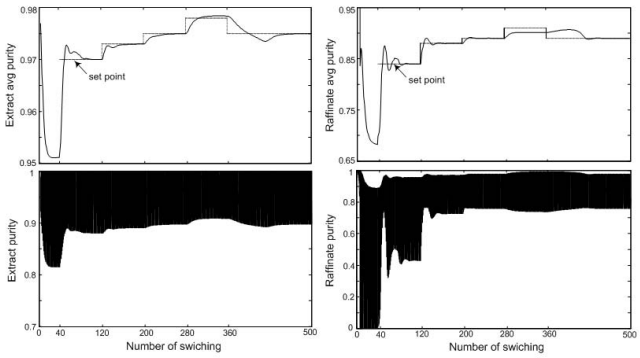

Fig. 2. Transient response of extract and raffinate purities under the successive increase in the purity set points.

where $y_{k|k-1}(N)$ represents the prediction of $y_k(N)$ based on the concentration measurements after the $k-1^{\text{th}}$ cycle. The Kalman filter for $y_{k|k-1}(N)$ is basically same as (8) except that the measurement update is conducted only once at $t = N$ for each cycle. Therefore, starting from $z_{k-1|k-1}(N)$, which is equivalent to $z_{k-1}(N|N)$ in (8), only the model update equation is repeated up to $z_{k|k-1}(N)$, which is equivalent to $z_{k-1}(2N|N)$ in (8), then the following measurement update is taken

$$z_{k|k}(N) = z_{k|k-1}(N) + K(t)(y_k(N) - C_k(N)z_{k|k-1}(N)) \tag{14}$$

Accordingly, $y_{k|k-1}(N)$ is given as a function of $\Delta u_k(0)$, $\cdots$, $\Delta u_k(N-1)$.

3.4 Results and discussion

The controller was implemented with two different model linearization strategies: use of repeatedly linearized model at every column switching and use of a fixed time-varying linear model, respectively. The performance of each strategy was investigated against set point tracking and step changes in the feed concentration and also in the equilibrium adsorption constants, respectively.

Purity improvement under repetitive control

Figure 2 demonstrates how the purities can be improved under repeated set point change by the proposed RC method from an open loop state. In the beginning, a pure separation condition was determined using Mazzotti's triangle method (Mazzotti et al., 1997) and applied for 40 column switchings until the cyclic steady state is reached. From then on, the purity set points for both extract and raffinate were increased incrementally. One can observe that the outputs smoothly follow the increasing set points until the extract and raffinate purities attain 0.975 and 0.89, respectively. When the set points are increased again to (0.978, 0.91), which is on the edge of the purity reachable region, the outputs fail to settle resulting in offset. As the set points are returned to the previous values, the purity regulation is restored without offset.

One can notice from Fig. 2 that the output overshoot is diminished as the purity set points are increased. This manifests the effects of the decreasing process gain despite the repeated renewal of the control model by successive linearization as the operating condition approaches to the

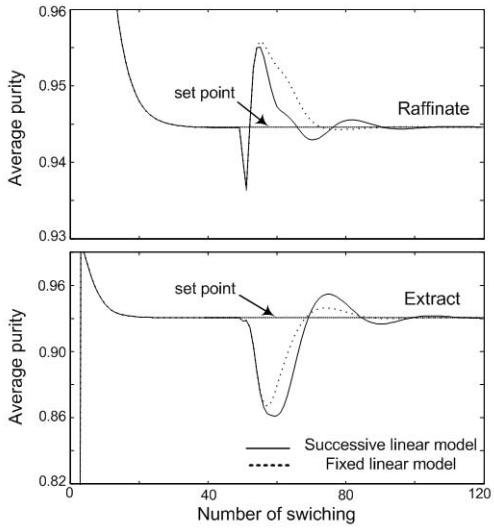

Fig. 3. Control performance against a step change in feed concentrations (c_A^{in}=0.5 → 0.3, c_B^{in}=0.5 → 0.7).

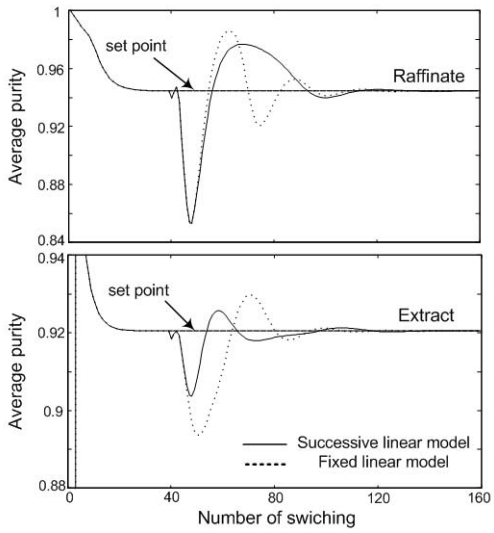

Fig. 4. Control performance against error in model parameter ($H_A = 3 \rightarrow 4.2$).

edge of the reachable region. Though not shown here, RC using a fixed model linearized at the initial cyclic steady state fails to track the first set point change and diverges.

Disturbance rejection

The regulatory performance of the RC method is investigated against a step change in the feed concentration. Figure 3 shows the closed-loop responses when c_A and c_B in the feed stream change from (0.5, 0.5) g/cm^3 to (0.2, 0.8) g/cm^3 stepwise from the 50$^{\text{th}}$ switching. Two RC's are compared: one with the successively linearized model and the other with a fixed model linearized around the state before the feed concentration change. Performance difference is not salient in this case, which can be anticipated since the fixed linear model can reasonably represent the local behavior around a steady state.

Robustness

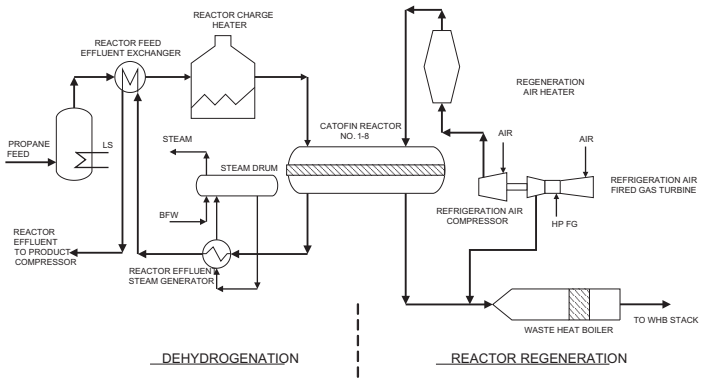

Fig. 5. Process flow diagram (a) and scheduling chart for multiple reactors (b) of the CATOFIN process.

In Fig. 4, the performance against model uncertainty is shown. H_A was changed from 3 to 4.2 from the 40$^{\text{th}}$ switching. Both RC methods recover the purities to their original set points after some transients. In this simulation, successive linearization-based RC performs better than fixed linear model-based RC producing less overshoot and shorter settling time although the performance difference is not significant as is in the set point change.

4. APPLICATION TO CATOFIN PROCESS

This part is from Seo et al. [2007].

4.1 Description of process and control problem

The CATOFIN process shown in Fig. 5 is a recently emerged propylene production process using catalytic dehydrogenation of propane. The reactor consists of multiple parallel adiabatic fixed-beds, where dehydrogenation (Dehyd) of propane and catalyst regeneration (Regen) by decoking are carried out alternatively over roughly ten minutes of period for each operation. During the Dehyd operation, bed temperature is gradually decreased by the endothermic reaction. The bed temperature is restored during the exothermic Regen period. Propylene can be produced continuously by exquisite scheduling of the multiple reactor beds. Individual catalyst beds in the reactor are under repetitive operation where the results of a previous cycle affect the operation of the upcoming cycle.

4.2 Process model

The following reactions are considered to take place in the CATOFIN reactor under adiabatic condition (Kim et al., 1980: Kern et al., 2005):

$$\left.\begin{aligned} &C_3H_8 \overset{k_1}{\underset{k_2}{\leftrightarrows}} C_3H_6 + H_2 \\ &C_3H_6 \xrightarrow{k_3} 3C + 3H_2 \\ &C_3H_8 + C_3H_6 \xrightarrow{k_4} 2CH_4 + C_2H_6 + 2C \end{aligned}\right\} \text{during Dehyd}$$

$$C + O_2 \xrightarrow{k_5} CO_2 \qquad \text{during Regen}$$

The reactor can be modeled by two sets of PDE's that describe unsteady state component balance and enthalpy

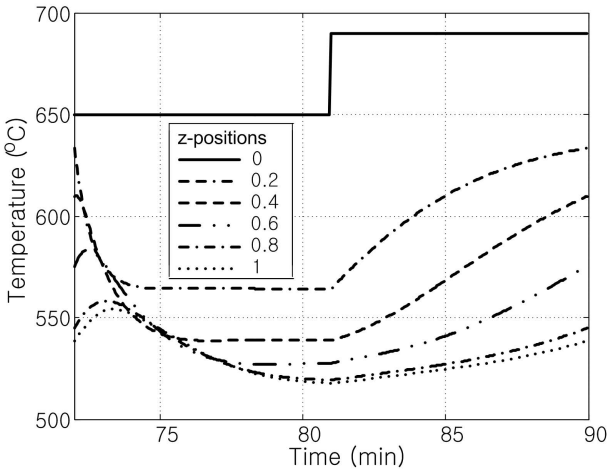

Fig. 6. Bed temperature trajectories at six axial positions under a periodic steady state.

balance for Dehyd and Regen periods, respectively. Similarly to the SMB process, the PDE models were reduced to ODE models by applying the CSCM.

Fig. 6 shows time-dependent trajectories of the bed temperatures at six collocation points during Dehyd and Regen cycles, respectively, after they reach a cyclic steady state. By the endothermic reaction, bed temperatures are decreased as the propane Dehyd proceeds, but restored by the heat of combustion during the Regen operation.

In the operation of the reactor, it was assumed that only the bed temperatures at the six collocation points are measured in real-time. Also it was assumed that the control action is taken during the Regen period whereas the Dehyd operation is carried out under an open-loop state. The purpose of control is to raise the first two of the six bed temperatures to the respective target values at the end of the period by manipulating the flow rate and temperature of the combustion air.

4.3 RC formulation

First, the ODE reactor models were converted to the following discrete-time equivalent model:

$$\begin{aligned} x_k(t+1) &= f(x_k(t), u_k(t)) \\ y_k^m(t) &= C^m x_k(t) \\ y_k(t) &= C x_k(t) \end{aligned} \tag{15}$$

with

$$f = \begin{cases} f^D, & t \in [0, t_{deh}] \\ f^R, & t \in [t_{deh}+1, N] \end{cases} \tag{16}$$

$$(x,u) = \begin{cases} (x^D, 0), & t \in [0, t_{deh}] \\ (x^R, [T_{air}\ q_{air}]), & t \in [t_{deh}+1, N] \end{cases}$$

where the superscripts ^{D} and ^{R} represent the Dehyd and Regen operations, respectively; N denotes the total sample number of a cycle; x represents the state that consists of the concentrations of the associated chemical species and the bed temperatures at the collocation points; y^m and y denote the six measured and two controlled bed temperatures, respectively; u represents the MV, which is void for Dehyd, but refers to the temperature and flow rate of the combustion air for Regen, respectively.

The states are carried over between Dehyd and Regen according to

$$\begin{aligned} x_k^R(t_{deh}+1) &= M x_k^D(t_{deh}) \\ x_{k+1}^D(1) &= P x_k^R(N) \end{aligned} \tag{17}$$

where M is a matrix that selects the bed temperatures and coke deposit from $\mathbf{x}_k^D(t_{dey})$ for transferring them to $\mathbf{x}_k^R(t_{dey})$ and resets the initial oxygen concentrations in $\mathbf{x}_k^R(t_{dey})$ to zero. P is defined in a similar way.

During the Dehyd period, only the state estimation is carried out since there is no control action. The extended Kalman filter (EKF) constructed on (15) was employed for this purpose. During the Regen cycle, the control action is taken. These two operations constitute one cycle operation of RC. For the formulation of the RC algorithm for Regen, the same procedure in section 2 can be applied to except that the control objective needs to be modified for end time control. Since the bed temperature measurements are available in real-time, the control problem can be recast to the following predictive control form:

$$\min_{\Delta u_k(\cdot)} \frac{1}{2} \left\{ \|r - y_k(N|t)\|_Q^2 + \sum_{t=0}^{N-1} \|\Delta u_k(t)\|_R^2 \right\} \tag{18}$$

$y_k(N|t)$ is the prediction of $y_k(N)$ based on the bed temperature measurements up to t and is given as a function of $\Delta u_k(t), \cdots, \Delta u_k(N-1)$. In summary, the operation of RC in one cycle can be stated by the following steps:

[step 1] Estimate $\mathbf{x}_k^D(t|t)$ during the Dehyd operation with the EKF constructed on (15) using $y^m(t)$.
[step 2] State transition from the Dehyd to Regen operations using the state transition rule in 18).
[step 3] At $t = t_{reg}$, solve (18) and determine $\Delta u_k(t_{reg})$, $\cdots, \Delta u_k(N-1)$. Implement $\Delta u_k(t_{reg})$ on the process.
[step 4] Repeat step 3 at $t+1$ and on until $t = N-1$.
[step 5] State transition to Dehyd in the next cycle using (18).

4.4 Results and discussion

Performance of the proposed RC has been investigated against a set point change. The set point was changed from [681.9°C 651.6°C], which is the output values at the terminal time of the Dehyd operation under the cyclic steady state with $u^R(t)$=[180 ton/h 690°C], to [690°C 660°C]. Besides this set point change, random (but fixed) errors of maximum 10% were imposed on the reaction rates in the nominal reactor model. In Fig. 7, the response of the bed temperatures at z=0.2, 0.4 at the end of Regen operation and the corresponding input changes are shown. It can be observed that the bed temperatures are subject to slight overshoot but settled in around 11 cycles. The resulting transient periods are only typical ones and they can be shortened or may be lengthened by the

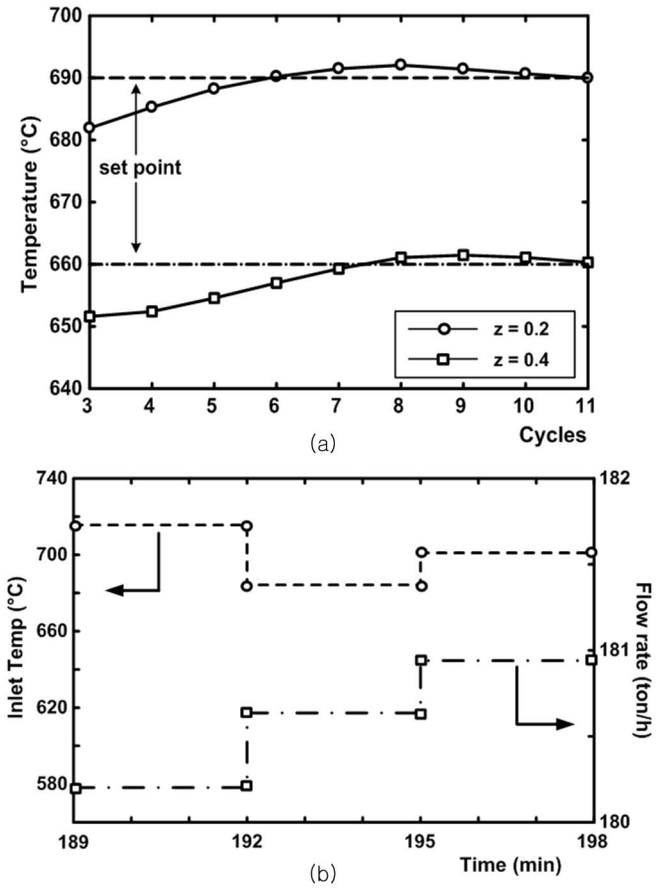

Fig. 7. Performance of RC to a set point change to [690°C 660°C]; (a) two controlled bed temperatures during the Regen operation, (b) input profiles.

weighting matrices in the quadratic objectives and also the covariance matrices for the Kalman filter.

5. CONCLUSIONS

Severe nonlinearity is common in chemical processes, especially where reaction and/or separation takes place. For such processes, performance of time-invariant linear model-based control methods may show limitations.

This paper describes a stochastic RC technique that is based on a successively linearized model of a nonlinear process with applications to two repetitive chemical processes, SMB and CATOFIN processes. A general framework for the stochastic RC method is shown first, and tailoring methods for each process according to the process characteristics and requirements are described.

Numerical simulation has shown that the proposed method is effective for nonlinear repetitive processes with random disturbances.

ACKNOWLEDGEMENTS

This work was supported by the KOSEF through the Center of Advanced Bioseparation Technology at Inha University and also by the Korea Energy Management Corporation. K. S. Lee also would like to acknowledge the financial support from the Korea Research Foundation through the Second Stage Brain Korea Program. JHL acknowledges the financial support from LGChem and Owens Corning.

REFERENCES

T. Inoue, M. Nakano, S. Iwai, High accuracy control of proton synchrotron magnet power supply, Proc. of IFAC 8th World Congress, Kyoto, (1981), 216-221.

T. Omata, M. Nakano, and T. Inoue, Applications of repetitive control method to multivariable systems, *Trans. of SICE*, 20(9), pages 795–800, 1984 (In Japanese).

S. Hara., Y. Yamamoto., T. Omata., N. Nakano., Repetitive control system: A new type servo system for periodic exogeneous signals. *IEEE Trans. A. C.*, 33, pages 659–668, 1988.

G. Weiss and M. Häfel, Repetitive control of MIMO systems using H^∞ design, *Automatica*, 35 pages 1185–1199, 1999.

M. Tomizuka, T. Tsao, K. Chew, Analysis and synthesis of discrete-time repetitive controllers, *Trans. of ASME, J. of Dynamic Systems, Measurement, and Control*, 111, pages 353–358, 1988.

R. W. Longman., Iterative learning control and repetitive control for engineering practice. *Int. J. Contr.*, 73, 10 pages 930–954, 2000.

J. H. Lee., S. Natarajan., and K. S. Lee., A model-based predictive control approach to repetitive control of continuous processes with periodic operations. *J. Process Control.*, 11, 195, 2001.

K. S. Lee, J. Lee, I. Chin, J. Choi, and J. H. Lee, Control of wafer temperature uniformity in rapid thermal processing using an pptimal iterative learning control technique. *Ind. Eng. Chem. Res.*, 40, 1661-1672, 2001.

W. Yun and K. S. Lee, The use of cubic spline and far-side boundary condition for the collocation solution of a transient convection-diffusion problem. *Korean J. Chem. Eng.*, 24(2), pages 204–208, 2007.

M. Mazzotti, G. Storti, and M. Morbidelli. Optimal operation of simulated moving bed units for nonlinear chromatographic separations, *J. Chromatogr. A*, 769, 3, 1997.

S. Seo, W. Won, K. S. Lee, and S. Lee, Repetitive control of CATOFIN process, *Korean J. Chem. Eng.*, 2007. *in press*

Y. G. Kim, H. S. Lee, and Y. S. Song, A study on dehydrogenation of propane. *Korean J. Chem. Eng.(in Korean)*, 18, pages 11–19, 1980.

C. Kern, and A. Jess. Regeneration of coked catalysis: modeling and verification of coke burn-off in single particles and fixed-bed reactors, *Chem. Eng. Sci.*, 60, 4249-4264, 2005.